Metallostructures

DOI: 10.1002/anie.200903185

Predesigned Hexanuclear Cu^{II} and Cu^{II}/Ni^{II} Metallacycles Featuring Six-Node Metallacoronand Structural Motifs**

Feng Li, Jack K. Clegg, Paul Jensen, Keith Fisher, Leonard F. Lindoy, George V. Meehan, Boujemaa Moubaraki, and Keith S. Murray*

The metal-ion-directed assembly of discrete molecular architectures, especially those with interesting supramolecular topologies, has received very considerable attention over recent years. The resulting metallostructures range from simple molecular ellipses, through higher polygons, to large polyhedrons with molecular weights of many thousands.[1] A condition for the rational assembly of such metal–organic structures is that the metal ion(s) and organic component(s) display the steric and electronic complementarity that is required to promote formation of the molecular architecture of interest.

In previous studies, we have investigated the synthesis of a range of neutral nanometer-scale metal–organic architectures that employ 1,3- and 1,4-aryl-linked bis(β-diketonate) dianions as the organic components. The products include a discrete tetranuclear cofacial 'dimer of dimers', dinuclear helicates, supramolecular tetranuclear tetrahedral structures, and a range of interesting extended structures, which also incorporate difunctional co-ligands that fall in the category of metal–organic framework materials.[2,3] It is clear both from our studies, as well as those of other research groups,[4,5] that bis(β-diketone) derivatives of the above type show uncommon utility as structural elements for the construction of interesting discrete and extended metal–organic architectures.

We report herein the results of a further investigation in which the assembly of new hexanuclear species of unprecedented structure has been achieved by the interaction of Cu^{II} alone or a combination of Ni^{II} and Cu^{II} with the 1,4-aryl-linked bis(β,δ-triketone) LH_4. The latter is the first example of a 1,4-aryl-linked bis(β,δ-triketone) ligand reported to date. While LH_4 may be considered a bis(β,δ-triketone) analogue of the corresponding 1,4-aryl-linked bis(β-diketone) species employed in our previous studies, it incorporates the capacity for coordination to two additional metal ions over the bis(β-diketone) species (that is, four ions in all), the pairs of which will be in proximity.

Several factors influenced our choice of LH_4 for use in this study. Although without direct precedence, individual ligands of this type are readily synthesized using chemistry that is well established by our research group. A strong affinity of the β,δ-triketonate units for metal ions across several areas of the periodic table was anticipated based on the known metal-ion chemistry of the corresponding simple β,δ-triketone ligands,[5] as well as of the corresponding 1,3-aryl-linked bis(β,δ-triketone) derivatives.[5,6] Furthermore, the ability of each β,δ-triketone unit to lose two protons upon metal complexation provides the opportunity for neutral metal complexes to be generated. As no additional anions additional are required, the equilibria involved in the assembly process are simplified, thus assisting the generation of the targeted molecular geometry. Furthermore, by analogy with the behavior of the above-mentioned 1,4-aryl-linked bis(β-diketonato) analogue towards Cu^{II}, and, as expected for the formation of an entropy-favored discrete product, it seemed likely that the coordination vectors of the β,δ-triketonato fragments in L^{4-} would be orientated in an aligned (that is, non-opposed) manner upon complex formation. This orientation, coupled with the restricted flexibility that arises from the fully sp^2 hybridized ligand backbone, was expected to generate a 'bent' geometry for L^{4-} on metal coordination (Figure 1). As expected, a molecular mechanics calculation[7] also confirmed the existence of an energy minimum for this essentially planar 'bent' ligand configuration.

Consideration of the coordination vectors in the above ligand arrangement reveals that if an uncharged discrete metal-containing product is to be generated, then the simplest least-strained neutral assembly will involve the interaction of six divalent metal ions with three L^{4-} ligands to yield a hexanuclear array in which all donor oxygen atoms and the metal centers occupy the same plane. The resulting structure corresponds to an unprecedented hexanuclear metallacoronand motif (**1**, Figure 1).

The preparation of LH_4 was based on the related synthesis of the corresponding 1,3-linked analogue[6] and involved a Claisen condensation between dimethyl terephthalate and 6-methyl-2,4-heptane-dione (the synthesis and characterization of LH_4, including its X-ray structure showing a *transoid* arrangement of the β,δ-triketone groups, is given in the Supporting Information).

[*] Dr. F. Li, Dr. J. K. Clegg, Dr. P. Jensen, Dr. K. Fisher, Prof. L. F. Lindoy
School of Chemistry, University of Sydney
Sydney, NSW, 2006 (Australia)
Fax: (+61) 2-9351-3329
E-mail: l.lindoy@chem.usyd.edu.au
Prof. G. V. Meehan
School of Pharmacy and Molecular Sciences, James Cook University
Townsville,QLD, 4811 (Australia)
Dr. B. Moubaraki, Prof. K. S. Murray
Department of Chemistry, Monash University
PO Box 23, VIC, 3800 (Australia)

[**] This research was supported by the Australian Research Council. We thank Dr. J. C. McMurtrie, J. Bouzaid, and Dr. T. Bostrom for experimental assistance at the QUT Analytical Electron Microscopy Centre, Brisbane.

Supporting information for this article is available on the WWW under http://dx.doi.org/10.1002/anie.200903185.

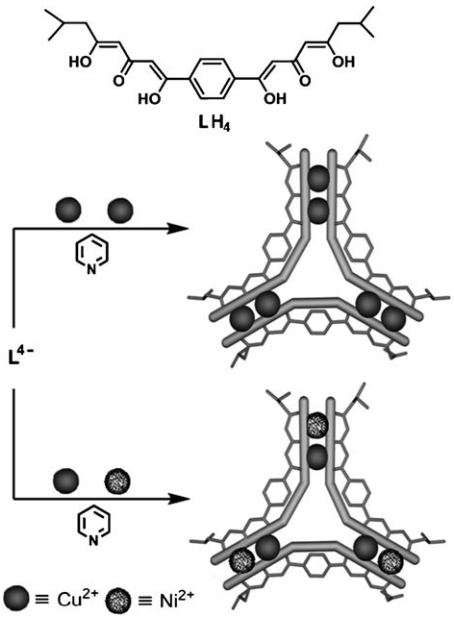

Figure 1. Structure of LH_4. Assembly of the hexanuclear metallacoronand metal clusters **1** (top) and **2** (bottom); coordinated pyridine solvate molecules are not shown in both cases.

Reaction of LH_4 with two equivalents of Cu^{II} acetate in a methanol/acetone mixture, followed by recrystallization of the product from pyridine and drying under vacuum for 48 hours, resulted in the formation of a dark-brown crystalline product **1**. The microanalytical data for **1** was in agreement with the anticipated stoichiometry of $[Cu_6L_3]$. The solid state UV/Vis spectrum of **1** exhibits a strong absorption, which is assigned to a charge-transfer transition, in the 400–500 nm region, while a broad absorption envelope at higher wavelength with $\lambda_{max} = 685$ nm is assigned to overlapping d–d transitions. The FTIR spectrum shows multiple absorptions in the region 1600–1500 cm^{-1}; these signals are typical of coordinated carbonyl groups and ethylenic bonds. The characteristic strong absorption at 1600 cm^{-1} observed for free LH_4 is absent in the spectrum of this complex, which is consistent with the metal coordination of all the carbonyl oxygen atoms. The MALDI-TOF mass spectrum contains peaks at m/z 1613.97 and 1635.85 (most abundant isotopic peaks), which correspond to the $[Cu_6L_3{+}H]^+$ and $[Cu_6L_3{+}Na]^+$ parent ion clusters, respectively (see Figure S2 in the Supporting Information), and are consistent with the expected metal/ligand ratio of 6:3.

Since two different metal-binding domains exist in $\mathbf{L}^{4-}$, an attempt was made to prepare a corresponding Cu^{II}/Ni^{II} derivative that is related to **1**, but contains nickel and copper in adjacent sites throughout the assembly. The stepwise reaction of LH_4 in THF/MeOH with one equivalent of copper(II) acetate, then one equivalent of nickel(II) acetate, and subsequent slow recrystallization of the product from pyridine gave a brown crystalline product. A single crystal (compound **2**) was removed directly from the pyridine solution and, after rapid handling at dry-ice temperature, was used for an X-ray structure determination (see below).

The remaining brown product from the crystallization was isolated by filtration and was subjected to CHN microanalysis after drying under vacuum for 48 hours. Based on the microanalysis results, the composition of the remaining product was initially assigned as $Cu_3Ni_3L_3{\cdot}5\,Py$; however, because of the similarity in atomic masses of nickel and copper, it is noted that this result is not useful for accurately defining the Cu/Ni ratio present (see below). The solid-state UV/Vis spectrum of the above product again exhibited a strong charge-transfer transition in the 400–500 nm region, while a broad d–d absorption envelope with $\lambda_{max} = 690$ nm, was also present at higher wavelengths. The FTIR spectrum was very similar to that of **1**; the characteristic strong absorption at 1600 cm^{-1} observed for free LH_4 was again absent in accord with the metal coordination of all the ligand carbonyl groups. However, the MALDI-TOF mass spectrum of this product is more complex than originally anticipated and shows a parent-ion peak region whose isotopic distribution appeared inconsistent with the presence of a single compound. Attempts at simulation of the parent-ion region of the spectrum (see Figure S3 in the Supporting Information) indicated that the observed pattern predominantly corresponded to a mixture of $[Cu_3Ni_3L_3{+}H]^+$ and $[Cu_4Ni_2L_3{+}H]^+$ ions, although the presence of small amounts of other ions from the series $[Cu_{(6-n)}Ni_{(n)}{+}H]^+$ ($n = 1$-3) could not be ruled out. Prompted by the above result, the Cu/Ni ratio in the above product was subsequently determined directly by inductively coupled plasma (ICP) analysis to be 1.53:1, rather than the 1:1 ratio required for the Cu_3Ni_3-containing product.

In view of the above results, a visual microscopic inspection and scanning electron microscopy–energy-dispersive spectroscopy (SEM-EDX) analysis were carried out. A sample of vacuum-dried $Cu_3Ni_3L_3{\cdot}5\,Py$ was redissolved in pyridine and the crystallization procedure was repeated. As before, the brown needle-like material that formed over 48 hours was isolated and immediately inspected, without drying, under a microscope. Two superficially related, but nevertheless clearly different, crystal habits were observed (see Figure S6 in the Supporting Information). The first crystal type underwent rapid decay (with loss of pyridine) on standing, while the second product (also brown) appeared to be air-stable. With cooling and rapid handling, the unit-cell dimensions of a single crystal of the former type were determined, and were the same as those obtained for **2**, thus confirming that both products were identical. In contrast, an attempted parallel X-ray investigation of the second product (with the more visually stable habit) found that it failed to diffract even when a significantly longer exposure time was employed.

For the SEM-EDX analyses, three crystals of each of the above products that showed different habits were separated with the aid of a microscope and three EDX measurements were taken on different regions of each sample to confirm uniformity; the as-measured variation was less than 5%. The crystals of **2** yielded a Cu/Ni ratio of 0.97:1, which provided confirmation that this product has the 1:1 Cu/Ni ratio initially anticipated when planning the 'two-metal/two-binding-domains' experiment discussed above.

The crystal structures of **1** and **2** (Figure S4 in the Supporting Information and Figure 2) confirm that the respective assemblies are uncharged hexanuclear metalla-

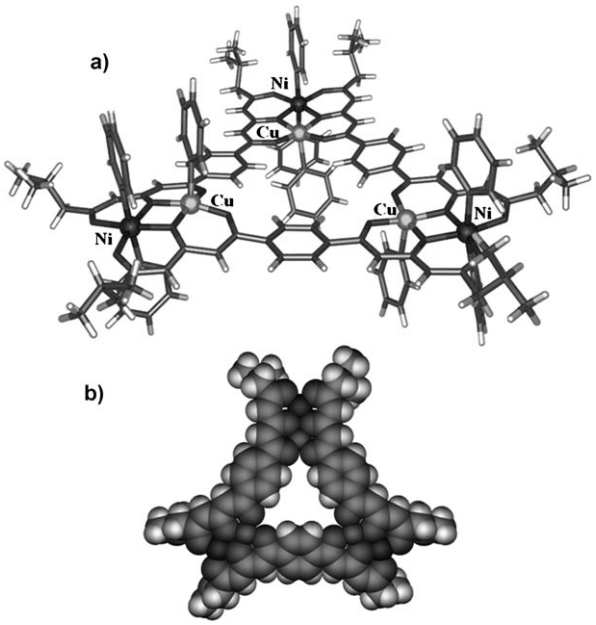

Figure 2. Structure of the hexanuclear complex $[Cu_3Ni_3L_3Py_9]\cdot 3.25\,py$ (**2**). a) Overall view of the molecule showing the coordinated pyridine co-ligands; pyridine solvate molecules are not shown. b) Space-filling view of the "in-plane" metallacoronand motif.

cycles (that incorporate the triketonato ligands in the bent configuration discussed earlier). Each metallacycle exhibits the 'in-plane' C_3-symmetric metallacoronand motif shown in Figure 1. The six metal centers in each structure constitute a near-planar array, in which the chelate rings and phenylene groups deviate only slightly from the respective mean planes (the latter presumably to reduce steric interference and/or to satisfy connectivity and packing requirements). In each structure, oxygen atoms occupy equatorial positions around each octahedral metal site; they also occupy the basal planes of the square-pyramidal sites while, with one exception, all axial and apical positions are occupied by either one or two pyridine co-ligands. When present in these species, six-coordination occurs at the "outer" metal centers in each case. Uncoordinated pyridine molecules are also present in the respective crystal lattices. Since the crystals of both **1** and **2** rapidly lost pyridine molecules when removed from pyridine solution, it was not unexpected that each of the resulting structures of **1** and **2** reflected 'partially desolvated' products.[8] The X-ray crystallographic results for **1** indicate a stoichiometry of $[Cu_6L_3Py_8]\cdot 6.25\,Py$, which is best modeled in the present study as corresponding to a product of type $\{[Cu_6L_3(Py)_8]_{0.75}[Cu_6L_3(Py')_8]_{0.25}\}\cdot 6.25\,Py$ in which 75% of the molecules contain two six-coordinate and four five-coordinate copper centers, while 25% have three six-coordinate centers, two five-coordinate centers, and one four-coordinate center. The two forms are thus structural isomers (the first of these is shown in Figure S5 in the Supporting Information). Each Cu^{II} ion is separated from the adjacent Cu^{II} ion by 3.03–3.04 Å, which is slightly larger than the sum of the Van der Waals radii for this ion. Adjacent complexes pack together along the crystallographic *b* axis to form a columnar arrangement that involves a number of π–π interactions (see Figure S5 in the Supporting Information).

The composition of $[Cu_3Ni_3L_3Py_9]\cdot 3.25\,Py$ for **2** was confirmed by the X-ray crystal structure of **2** and the 1:1 Cu/Ni ratio obtained in the EDX study. It is noted that the brown crystals isolated for **2** also crystallized in a different space group to that of **1**. The X-ray structure shows an assembly of type $[Ni_3Cu_3L_3Py_9]\cdot 3.25\,Py$. The three outer Ni^{II} centers show normal (high-spin) octahedral coordination, while the three (inner) Cu^{II} centers adopt approximate square-pyramidal geometries (Figure 3), which is also a

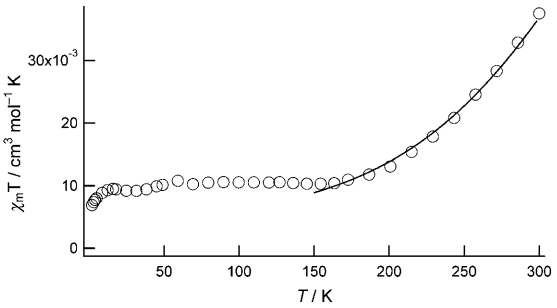

Figure 3. Plot of $\chi_M T$ per Cu^{II} ion versus temperature for **1**, $[Cu_6L_3]$. The solid line is the best fit plot using the parameters given in the text.

common geometry for this ion. No evidence for any other arrangement of these metal centers was observed. Each of the two adjacent metal ions is separated by 3.06–3.07 Å. Overall, the crystal packing for **2** is similar to that observed for **1**, with, once again, uncoordinated pyridine molecules incorporated into the crystal lattice.

Finally, a variable-temperature investigation of the magnetic behavior of the fully desolvated form of **1**, $[Cu_6L_3]$, was undertaken.[9] We assumed that no coupling occurred across the aromatic spacers, and thus that the compound behaves as three independent $\{Cu_2(triketonato)_2\}$ groups. The plot of $\chi_M T$ per Cu^{II} ion is shown in Figure 3. The $\chi_M T$ value of $0.038\,cm^3\,mol^{-1}\,K$ ($0.55\,\mu_B$ per Cu^{II}) at 300 K, is greatly reduced from the uncoupled value because of very strong antiferromagnetic coupling. A gradual decrease occurs as the temperature is lowered so that a plateau value of approximately $0.01\,cm^3\,mol^{-1}\,K$ ($0.28\,\mu_B$ per Cu^{II} ion) is reached below about 150 K, this Curie-like behavior (150 to 2 K) is due to a combination of temperature-independent paramagnetic susceptibility (TIP; $60\times 10^{-6}\,cm^3\,mol^{-1}$ per Cu^{II} ion) and a paramagnetic monomer impurity of about 5%.

Population of the $S=0$ ground state below about 150 K for each antiferromagnetically coupled $\{Cu_2(triketonate)_2\}$ group, and thus also for the weakly linked hexanuclear cluster, has also been previously observed for isolated $\{Cu_2(triketonato)_2\}$ compounds.[10] This strong coupling arises from the efficient superexchange pathways that arise from overlap of the two coplanar $Cu(d_{x^2-y^2})$ 'magnetic

orbitals' and the p orbital on the central oxygen atom of each triketonate. Fitting of the susceptibility data to the Bleaney–Bowers $S = {}^1/_2$ dimer ($-2J\mathbf{S_1S_2}$) equation[11] gave best-fit parameter values; $g = 2.1$, $J = -460\ cm^{-1}$, $TIP = 60 \times 10^{-6}\ cm^3 mol^{-1}$, estimated monomer impurity = 5%. As indicated above, the J value compares very well to those reported for isolated, dinuclear $[Cu_2(triketonato)_2]$ species.[10] There is no evidence for any spin coupling between the Cu_2 pairs within the hexanuclear clusters, but such coupling would be hard to detect in view of the very weak susceptibilities observed.

In summary, examples of the self-assembly of two novel hexanuclear metallacoronand motifs from predesigned building blocks are described. The assemblies provide rare examples of both homo- and heterometallic architectures that incorporate multiple pairs of closely spaced metal ions. The adjacent metal centers of the hexanuclear copper species have been demonstrated to exhibit a strong antiferromagnetic interaction.

Experimental Section

$[Cu_6L_3]$ **(1)**: Copper(II) acetate monohydrate (96 mg, 0.48 mmol) in methanol (10 mL) was added dropwise to a warm (50 °C) solution of LH_4 (100 mg, 0.24 mmol) in acetone (50 mL). The mixture was stirred at 50 °C for 1 h, during which time the color changed to brown-green and some precipitate formed. The suspension was stirred for a further 15 h at room temperature. The solvent volume was reduced to 10 mL and the solid product present was isolated by filtration. Recrystallization from pyridine gave dark-brown microcrystals, which were isolated by filtration and dried under vacuum. Yield: 87 mg (67.4%). A crystal from the pyridine solution was used directly for the X-ray structure determination. On removal from the mother solution the crystal rapidly lost pyridine in air. Drying this product under vacuum for 48 h resulted in the complete loss of pyridine (confirmed by the absence of nitrogen in the CHN analysis of this product). IR (KBr pellets): $\tilde{\nu} = 2955, 2868, 1556, 1521, 1454, 1440, 1404, 1381, 1178, 991, 801\ cm^{-1}$; UV/Vis (THF): $\lambda_{max} = 447, 476, 685$ nm; MALDI-TOF MS (TCNQ) $m/z = 1613.97\ [M+H]^+$, 1635.85 $[M+Na]^+$. Elemental analysis calcd (%) for $C_{72}H_{78}Cu_6O_{18}$: C 53.62, H 4.88; found: C 53.84, H 5.03.

$[Cu_{(6-n)}Ni_{(n)}L_3]\cdot 6\,Py$ ($n = 1$–3): Cu^{II} acetate monohydrate (48 mg 0.24 mmol) was added to a cold (0 °C) solution of LH_4 (100 mg 0.24 mmol) in THF (70 mL). The mixture was stirred at 0 °C until the green solution just turned cloudy (ca. 15 min). At this point, nickel(II) acetate tetrahydrate (60 mg 0.24 mmol) in methanol (5 mL) was added and the resulting mixture was stirred overnight at room temperature. The solvent was removed, and the remaining yellow-green crude product was washed with methanol then acetone and dried under vacuum. Recrystallization of the product from pyridine gave brown microcrystals with a metallic appearance, which were isolated by filtration and dried under vacuum for 48 h. IR (KBr pellets): $\tilde{\nu} = 2956, 2869, 1563, 1522, 1454, 1437, 1294, 1179, 991, 805\ cm^{-1}$; UV/Vis (solid state): $\lambda_{max} = 428, 481, 690$ nm. The mass spectra (see Supplementary Information), EDX, and macrocyclic results indicated that this product consisted of a mixture of Cu/Ni species of type $[Cu_{(6-n)}Ni_{(n)}L_3]\cdot 6\,Py$ ($n = 1$–3), with the predominant species corresponding to $n = 3$ and $n = 2$. The calculated analytical data for all such species is similar; for simplicity only the calculated values for $[Cu_3Ni_3L_3]\cdot 6\,Py$ are listed here. Elemental analysis calcd (%) for $C_{72}H_{78}Cu_3Ni_3O_{18}\cdot 5\,py$: C 58.44; H 5.21, N 3.51; found: C 58.29, H 5.31, N 3.78. Yield: 70 mg (43.9%). A single crystal of **2** (see main text) taken directly from the pyridine solution was used for the X-ray structure determination; since the crystal rapidly lost pyridine in air, it was quickly transferred to the diffractometer and quenched with the nitrogen cryostream. The X-ray study (coupled with the 1:1 Cu/Ni ratio obtained for this product in the EDX study) confirmed a composition of $[Cu_3Ni_3L_3Py_9]\cdot 3.25\,py$ for **2**.

The Supporting Information contains additional experimental details of the X-ray, EDX, and magnetic and mass spectral determinations. CCDC 694102 (LH_4), 694103 (**1**) and 694104 (**2**) contain the supplementary crystallographic data for this paper. These data can be obtained free of charge from The Cambridge Crystallographic Data Centre via www.ccdc.cam.ac.uk/data_request/cif.

Received: June 12, 2009
Published online: August 17, 2009

Keywords: copper · magnetic properties · metallacoronands · metallacycles · nickel

[1] a) J.-M. Lehn, *Supramolecular Chemistry*, VCH, **1996**; b) M. Fujita, *Chem. Soc. Rev.* **1998**, *27*, 417–425; c) J. W. Steed, J. L. Atwood, *Supramolecular Chemistry*, VCH, New York, **2000**; d) L. F. Lindoy, I. M. Atkinson, *Self-Assembly in Supramolecular Systems*, Royal Society of Chemistry, Cambridge, **2000**; e) R. M. Yeh, A. V. Davis, K. N. Raymond in *Comprehensive Coordination Chemistry II*, *Vol. 7* (Eds.: J. A. McCleverty, T. J. Meyer), Elsevier, Oxford, **2004**, pp. 327–355; f) S. R. Seidel, P. J. Stang, *Acc. Chem. Res.* **2002**, *35*, 972–983; g) M. Tominaga, K. Suzuki, M. Kawano, T. Kusukawa, T. Ozeki, S. Sakamoto, K. Yamaguchi, M. Fujita, *Angew. Chem.* **2004**, *116*, 5739–5743; *Angew. Chem. Int. Ed.* **2004**, *43*, 5621–5625; h) F. Würthner, C.-C. You, C. R. Saha-Moller, *Chem. Soc. Rev.* **2004**, *33*, 133–146; i) M. Fujita, M. Tominaga, A. Hori, B. Therrien, *Acc. Chem. Res.* **2005**, *38*, 369–378; j) G. Seeber, B. E. F. Tiedemann, K. N. Raymond, *Top. Curr. Chem.* **2006**, *265*, 147–183; k) J. R. Nitschke, *Acc. Chem. Res.* **2007**, *40*, 103–112; l) E. R. Kay, D. A. Leigh, F. Zerbetto, *Angew. Chem.* **2007**, *119*, 72–196; *Angew. Chem. Int. Ed.* **2007**, *46*, 72–191; m) P. Mal, D. Schultz, K. Beyeh, K. Rissanen, J. Nitschke, *Angew. Chem.* **2008**, *120*, 8421–8425; *Angew. Chem. Int. Ed.* **2008**, *47*, 8297–8301; n) R. W. Saalfrank, H. Maid, A. Scheurer, *Angew. Chem.* **2008**, *120*, 8924–8956; *Angew. Chem. Int. Ed.* **2008**, *47*, 8794–8824.

[2] a) J. K. Clegg, L. F. Lindoy, B. Moubaraki, K. S. Murray, J. C. McMurtrie, *Dalton Trans.* **2004**, 2417–2423; b) J. K. Clegg, L. F. Lindoy, J. C. McMurtrie, D. Schilter, *Dalton Trans.* **2005**, 857–864; c) J. K. Clegg, L. F. Lindoy, J. C. McMurtrie, D. Schilter, *Dalton Trans.* **2006**, 3977–3984; d) D. J. Bray, J. K. Clegg, L. F. Lindoy, J. C. McMurtrie, D. Schilter, *Adv. Inorg. Chem.* **2006**, *59*, 1–37; e) J. K. Clegg, *Aust. J. Chem.* **2006**, *59*, 660; f) J. K. Clegg, D. J. Bray, K. Gloe, K. Gloe, M. J. Hayter, K. A. Jolliffe, G. A. Lawrance, G. V. Meehan, J. C. McMurtrie, L. F. Lindoy, M. Wenzel, *Dalton Trans.* **2007**, 1719–1730; g) D. J. Bray, K. A. Jolliffe, L. F. Lindoy, J. C. McMurtrie, *Tetrahedron* **2007**, *63*, 1953–1958; h) J. K. Clegg, D. J. Bray, K. Gloe, K. Gloe, K. A. Jolliffe, G. A. Lawrance, L. F. Lindoy, G. V. Meehan, M. Wenzel, *Dalton Trans.* **2008**, 1331–1340.

[3] D. J. Bray, B. Antonioli, J. K. Clegg, K. Gloe, K. Gloe, K. A. Jolliffe, L. F. Lindoy, G. Wei, M. Wenzel, *Dalton Trans.* **2008**, 1683–1685.

[4] For selected examples of bis(β-diketonates) and their complexes, see: a) A. P. Bassett, S. W. Magennis, P. B. Glover, D. J. Lewis, N. Spencer, S. Parsons, R. M. Williams, L. De Cola, Z. Pikramenou, *J. Am. Chem. Soc.* **2004**, *126*, 9413–9424; b) D. V. Soldatov, A. S. Zanina, G. D. Enright, C. I. Ratcliffe, J. A. Ripmeester, *Cryst. Growth Des.* **2003**, *3*, 1005–1013; c) D. V. Soldatov, *J. Chem. Crystallogr.* **2006**, *36*, 747–768; d) D. J. Bray, J. K. Clegg, L. F. Lindoy, D. Schilter, *Adv. Inorg. Chem.* **2006**, *59*, 1–37; e) M. Albrecht, S. Dehn, S. Schmid, M. DeGroot, *Synthesis* **2007**, 155–

158; f) E. C. Sañudo, T. Cauchy, E. Ruiz, R. H. Laye, O. Roubeau, S. J. Teat, G. Aromí, *Inorg. Chem.* **2007**, *46*, 9045 – 9047; g) R. W. Saalfrank, C. Spitzlei, A. Scheurer, H. Maid, F. W. Heinemann, F. Hampel, *Chem. Eur. J.* **2008**, *14*, 1472 – 1481.

[5] G. Aromi, P. Gamez, J. Reedijk, *Coord. Chem. Rev.* **2008**, *252*, 964 – 989.

[6] R. L. Lintvedt, J. K. Zehetmair, *Inorg. Chem.* **1990**, *29*, 2204 – 2209; R. L. Lintvedt, W. E. Lynch, J. K. Zehetmair, *Inorg. Chem.* **1990**, *29*, 3009 – 3013.

[7] Spartan 04, Wavefunction, Inc., Irvine, CA.

[8] Despite rapid handling at dry-ice temperatures, quenching in the nitrogen cryostream, long exposure times, multiple recrystallization attempts, and the use of a high-power laboratory source (5 kW from a rotating anode), the data obtained was less than ideal, with only reflections to ca. 1.0 Å resolution being recorded. The structure contains regions of disorder, and as a result, a number of constraints and restraints (including as rigid bodies) were required to facilitate realistic modeling of both species.

[9] Owing to difficulty in controlling the degree of pyridine present in the mixed Cu^{II}/Ni^{II} assembly **2**, no magnetic results are reported for this assembly.

[10] M. J. Heeg, J. L. Mack, M. D. Glick, R. L. Lintvedt, *Inorg. Chem.* **1981**, *20*, 833 – 839.

[11] B. Bleaney, K. D Bowers, *Proc. R. Soc. London Ser. A* **1952**, *214*, 451 – 465.

